The Effect of Residual Stresses Induced by Strain Peening upon Fatigue Strength

R. L. MATTSON AND J. G. ROBERTS
Research Laboratories, General Motors Corporation, Warren, Michigan

ABSTRACT

The purpose of this experiment was to determine the role of residual stresses in fatigue strength independent of other factors usually involved when residual stresses are introduced. It consisted of an investigation of the influence of residual stresses introduced by shot peening on the fatigue strength of steel (Rockwell C hardness 48) in unidirectional bending. Residual stresses were varied by peening under various conditions of applied strain. This process introduced substantially the same amount and kind of surface cold working with residual stresses varying over a wide range of values. Good correlation was found between residual stresses and fatigue strength tending to substantiate the concept of superpositioning of residual stresses and load stresses. It was also found that shot peening of steel of this hardness is beneficial primarily because of the nature of the macro residual stresses introduced by the process. There is no gain attributable to "strain hardening" for this material. An effort was made to explain the results on the basis of three failure criteria: distortion energy, maximum shear stress, and maximum stress.

INTRODUCTION

In the study of fatigue strength of materials, the experimental determination of the role of residual stresses as compared with load stresses has always been difficult because generally any method of introducing residual stresses also introduces other changes which independently might affect fatigue strength[1] (for example, changes in structure). It was the objective of this experiment to separate residual stresses from these other factors, and to study their significance to fatigue strength. The basis for the experiment is strain peening[2] and follows a suggestion made by J. O. ALMEN some years ago[3]. This technique permitted the introduction of a wide range of macro residual stresses near the surface of specimens by surface cold working in such a way that the "strain hardening" remained substantially constant. Fatigue tests and residual stress analyses were made of several groups of specimens and these showed good correlation between residual stress near the

References p. 357.

surface and the endurance limits. The experiment also served to clarify questions about the relative roles of "strain hardening" and residual stresses in the improvements in fatigue strength obtained by local cold-working operations such as shot peening and surface rolling.

EXPERIMENTAL

Specimens

Material. Specimens were machined from hot-rolled SAE 5160 spring steel of 0.215-in. thickness and 1-3/4-in. width.

Machining and heat treatment. Fatigue test specimens were prepared as follows: The material was:

(a) Normalized (1675 °F for 1-1/2 h).
(b) Specimens were machined to dimensions shown by Fig. 1 (equal amounts removed from opposite faces by shaping and grinding).
(c) Austenitized (15 min in rectified salt at 1600 °F).
(d) Quenched in oil.
(e) Pretempered (480 °F for 1 h).
(f) Tempered (770 °F for 2 h between clamped plates and air-cooled).

The resulting surface hardness, as measured by Rockwell C scale, was 48 ± 2. The resulting martensitic microstructure had some ferrite grains extending in places to a depth of 0.0004 in.

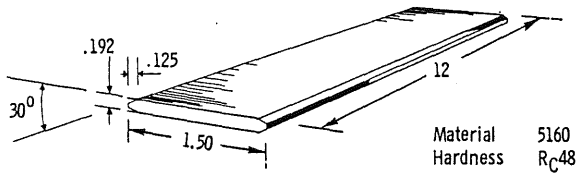

Fig. 1. Leaf-spring fatigue test specimen.

Presetting. After heat treatment and prior to shot peening, the specimens were given a conventional (in the spring industry) presetting operation. This was accomplished by means of curvature blocks and a hydraulic press. The curvature of these blocks was such that the curvature change from the free, flat condition (as heat treated) to the preset curvature was sufficient to stress the central 6 in. of length to a nominal surface stress of 220 k.s.i. (pounds per square inch, in thousands) which is slightly above the yield strength. This maximum stress was held for one-half minute. All presetting was in the same direction as the subsequently applied fatigue stress.

Shot peening. The strain-peening process is illustrated by Fig. 2. To the left,

References p. 357.

compressive strain peening is shown. Here the specimen is held under a condition of longitudinal bending to a fixed curvature with the test surface subjected to a compressive strain during the actual shot-peening operation. At the right, tensile strain peening is illustrated.

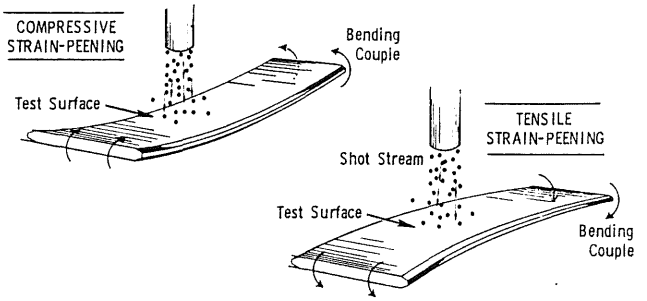

Fig. 2. Illustration of strain-peening process.

During peening, severe plastic flow occurs in a thin surface layer, upsetting the elastic strains due to the initial bending couple. The material beneath the thin surface layer remains unaffected by the peening. Upon release of the specimen from its holding fixture, relaxation occurs. The amount and direction of the relaxation depends upon the applied strain during peening. Hence, the magnitude of the resulting residual stress becomes a function of the applied strain during peening. For example, under conditions of tensile strain peening higher residual compressive stresses are introduced than peening under a "free" condition. Furthermore, tensile stresses can be introduced by shot peening under compression if the applied compressive strain is sufficiently high.

The shot peening was done in an air-type machine designed especially for experimental work. Four specimens were held in a fixture which was rotated and traversed beneath a fixed shot-nozzle. A single shot-peening treatment was used for all peening done in this experiment. SAE 230 chilled iron shot, 0.006 C Almen intensity, and full visual coverage was used. Only the "test surface" was peened (the surface later subjected to tensile strains during fatigue testing).

Specimen groups. The groups of specimens studied are listed in Table I. The "as heat treated" group was included for reference and comparison with the "preset only" group. The "preset only" group serves as a baseline since all shot-peened groups were preset prior to shot peening. The various shot-peened groups have the same amount of work hardening but differ in residual stress. The final group was included to obtain some measure of the influence of surface roughness as produced by shot peening on the fatigue strength. No additional surface treatment, other than that listed in Table I, was used.

References p. 357.

TABLE I

LIST OF TYPES OF SPECIMENS INVESTIGATED

As heat treated
Preset only
Conventionally shot peened
Shot peened under strain + 0.60 percent (180 k.s.i.)
,, ,, ,, ,, + 0.30 ,, (90 k.s.i.)
,, ,, ,, ,, — 0.30 ,, (−90 k.s.i.)
,, ,, ,, ,, — 0.60 ,, (−180 k.s.i.)
,, ,, free and stress-relieved for 2–1/2 h at 650 °F.

The longitudinal curvature of each specimen was measured with an arc-height gage (sensitivity 0.0001 $inch^{-1}$, curvature) after heat treatment, after presetting, and after shot peening. Curvature that causes tension stress on the test surface was taken as positive. Average specimen curvature after strain peening was dependent upon the magnitude and sign of the applied strain during peening. Curvature data are given in Table II.

TABLE II

LONGITUDINAL CURVATURE CAUSED BY PRESETTING AND STRAIN PEENING

Specimen state	*Average specimen curvature, $inch^{-1}$*
After heat treatment	0.0000
After presetting	+0.0010
After strain peening (+0.60%)	+0.0145
After strain peening (+0.30%)	+0.0100
After shot peening (conventional)	+0.0062
After strain peening (−0.30%)	+0.0005
After strain peening (−0.60%)	−0.0060

Photographs of the presetting equipment and of the curvature gage were presented in a previous paper[4].

Metallurgical examination. Micrographs and hardness–depth curves in the vicinity of the test surface were made on individual specimens in order to evaluate the extent of work hardening. Hardness was determined by means of a Tukon tester with 1000 g load and a diamond pyramid indentor. Results are shown by Fig. 3 and Fig. 4.

Surface roughness. The shot-peened test surface roughness was measured and surface profiles determined on a "Talysurf" machine. These results are summarized in Fig. 5.

Fatigue testing. One-directional bending type fatigue testing was used. All test-

References p. 357.

0.0004 in. partial decarburization

Preset only

58–59 4% Nital 500×
Specimen 255P-3

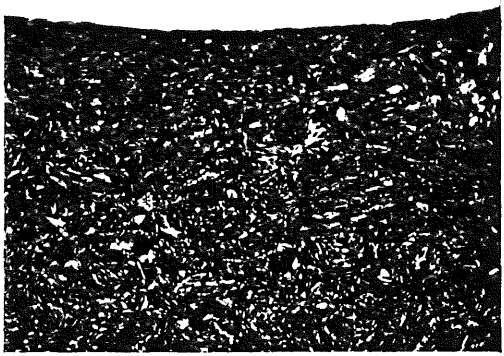

0.0012 grain distortion

Conventionally shot peened

58–58 4% Nital 500×
Specimen 301P-6

Fig. 3 (a). Micrographs of fatigue test tension surface of lengthwise cross-section. Preset only (upper), conventionally shot peened (lower).

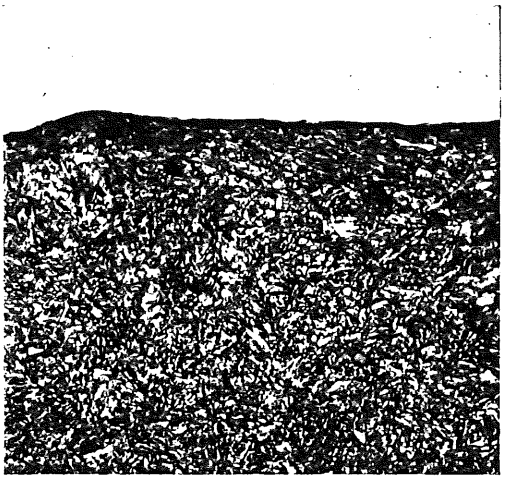

0.001 grain distortion

+0.60% strain peened

58–56 4% Nital 500×
Specimen 305P-8

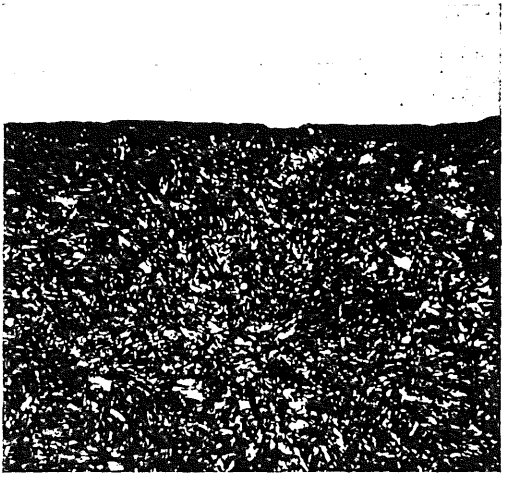

−0.60% strain peened

58–61 4% Nital 500×
Specimen 304P-3

Fig. 3 (b). + 0.60% strain peened (upper), −0.60% strain peened (lower).

ing was done on constant-deflection type machines (Fig. 6), operating at either 480 or 720 load cycles per minute. Surface stresses were calculated from longitudinal curvature changes and the flexure formula. These were verified by both static and dynamic strain gage (electrical resistance type) measurements. Load stress was

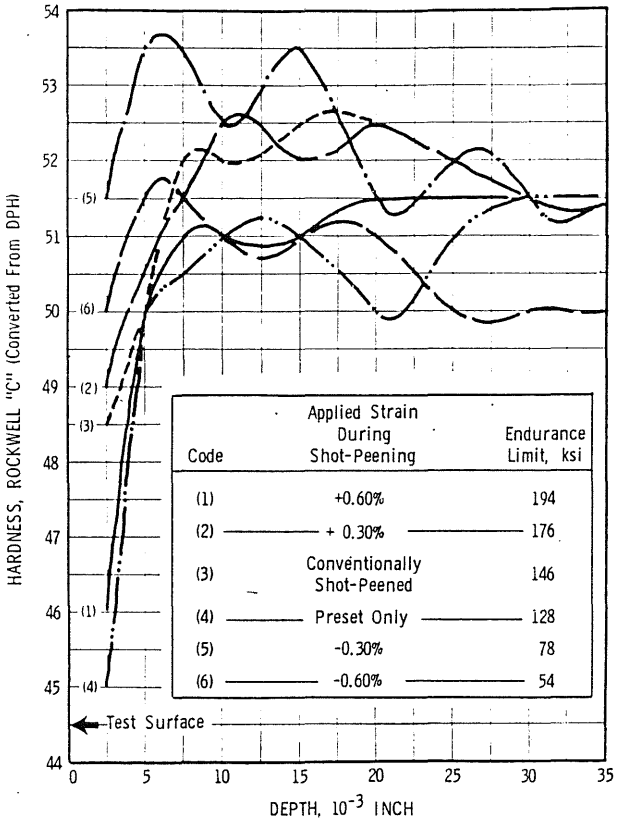

Fig. 4. Hardness–depth distributions.

applied by means of a curvature block attached to a movable beam which was driven in fixed vertical motion by a motor-driven shaft, with an eccentric operating a connecting rod. The other end of the beam was pin-connected to a fixed lower member on which two end blocks were attached, which supported the ends of the specimen. Each fatigue specimen was set up so that the specimen and curvature block were just into contact at the top of the stroke, and at the full vertical deflection the specimen and curvature block were in full contact through the central 6–in. length of the specimen. Transverse stresses caused by the loading cycle were approximately zero over the entire test region, as determined by resistance-type strain

References p. 357.

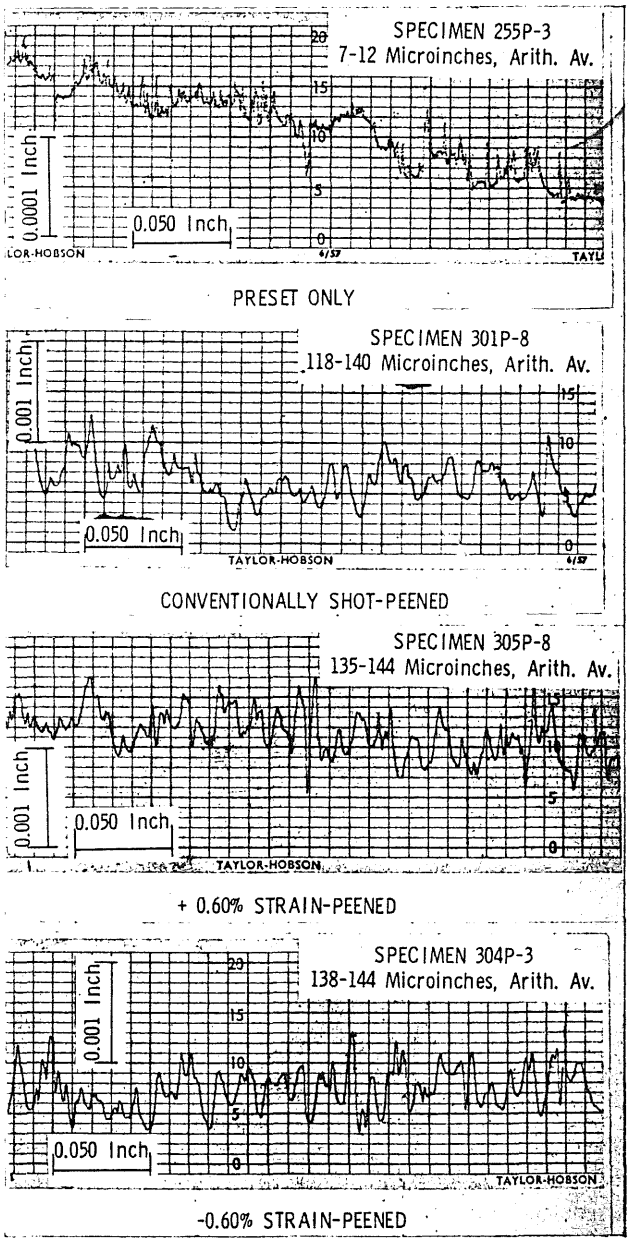

Fig. 5. Profiles and roughness measurements of test surfaces.

gages, assuming a Poisson's ratio of 0.3. A light-weight, straight motor oil was used to lubricate the frictional areas between the curvature block and the specimen and between the end blocks and the specimen. After an initial 10,000 stress cycles, each

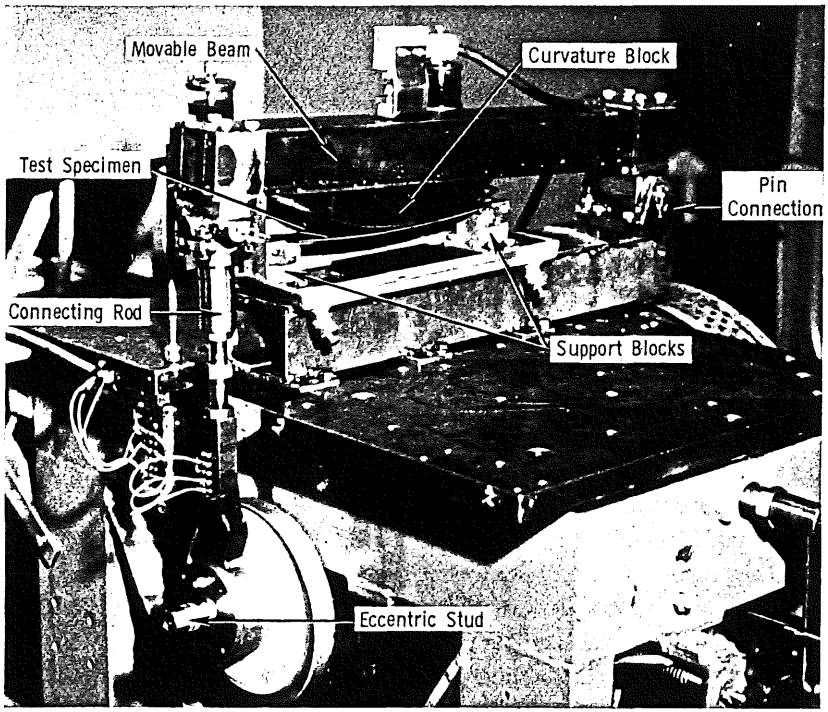

Fig. 6. Constant-deflection fatigue test machine.

specimen was removed from the fatigue test machine, and longitudinal curvature was measured and compared to the initial curvature. Any appreciable change in longitudinal residual stress caused by these stress cycles would be detected in this manner. Results of all fatigue tests, including curvature changes and locations of failure, are given by Appendix I.

Residual stress measurement. Macro residual stresses were measured using the "beam dissection" technique developed in our laboratory. Essentially, this technique consists of analyzing a small rectangular cross-section beam segment of the fatigue specimen by careful removal of a series of thin layers and measuring the changes in longitudinal curvature. A careful grinding technique was used to remove the thin layers. The layers ranged in thickness from 0.001 to 0.020 in., with the thinner layers removed in the most important regions. The basic equation employed is as follows:

References p. 357.

$$S_0(z) = \frac{E}{6}(t-z)^2 C'(z) - \frac{2E}{3}(t-z)C(z) + \frac{E}{3}\int_0^z C(z)\,dz,$$

where $S_0(z)$ = original longitudinal residual stress at depth z,
E = Young's Modulus,
t = specimen's original thickness,
z = depth of metal removed from original thickness,
$C(z)$ = specimen longitudinal curvature after removal of "z" material, and
$C'(z)$ = derivative of $C(z)$ with respect to z.

After obtaining the $C(z)$ curve, $S_0(z)$ was computed by an IBM 704 digital computer program for various values of z, and a longitudinal residual stress–depth curve was drawn.

A more complete description of the technique is given elsewhere[5]. This theory considers stresses in one direction only. Stresses perpendicular to the surface were taken to be zero.

The segments parted out from the fatigue specimens for residual stress analysis were 0.120 × 0.192 × 3 in. for longitudinal stresses and 0.060 × 0.192 × 1.5 in. for transverse stresses.

The residual stress distribution given in subsequent figures are those found in the individual segments. It is estimated that the error in the residual stress measurements of the segments was less than ± 5 k.s.i. A study was made of the error in these stresses due to the release of transverse stresses in the segments upon removal from the plate following the method described by JOHNSON[6]. It was found that the use of this correction was unnecessary for the purpose of this study.

One of the limitations of the techniques used is the lack of absolute measurements of stresses at the surface because of the removal of layers of finite thickness. Values referred to as being "near the surface" are actually those obtained from our measurement at a point 0.001 in. below the surface.

RESULTS AND DISCUSSION

Effect of presetting

Since all of the specimens were preset prior to shot peening, consideration will first be given to the influence of this operation on fatigue strength and residual stresses. The effect of presetting on residual stresses can be seen in the upper-right diagram of Fig. 7, which shows residual stress *vs.* depth for the first 0.025 in. from the test surface. It can be seen that presetting introduces about 35 k.s.i. compressive stress near the surface and the "as heat treated" specimen has a residual stress in this same region of about 5 k.s.i. tension. The improvement in fatigue

References p. 357.

strength caused by presetting is shown on the left. Surface roughness and hardness were about the same in both cases. This improvement can be attributed to the more favorable residual stress distribution. However, strain hardening cannot be ruled out completely. "Preset only" specimens will serve as our baseline for subsequent discussion.

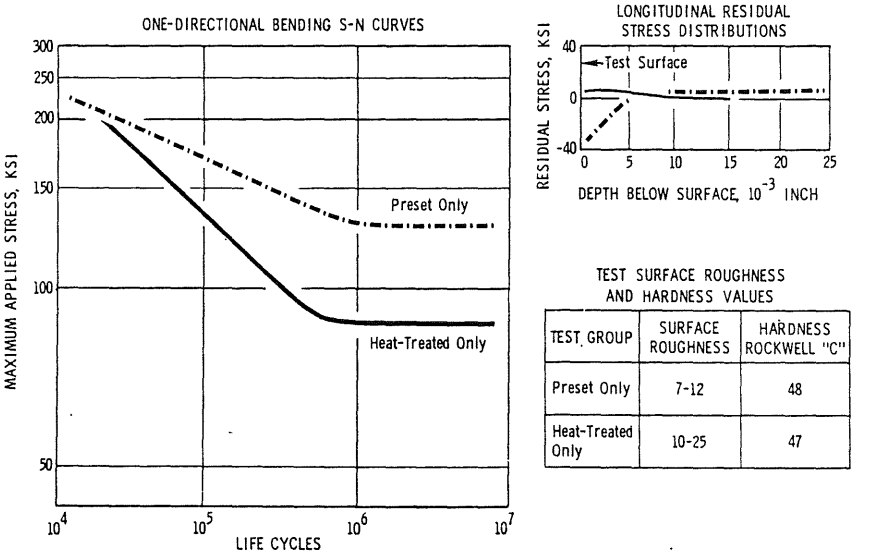

TEST SURFACE ROUGHNESS AND HARDNESS VALUES

TEST GROUP	SURFACE ROUGHNESS	HARDNESS ROCKWELL "C"
Preset Only	7-12	48
Heat-Treated Only	10-25	47

Fig. 7. Influence of presetting on bending fatigue strength.

Effect of strain peening

The effect of variable residual stresses and constant strain hardening (shot-peened specimens) on fatigue properties is illustrated by Fig. 8. To the left are S–N curves for six categories of specimens, and to the right are corresponding longitudinal residual stress distributions. The endurance limit of the preset specimen is approximately 128 k.s.i. and its residual stress near the surface is about 35 k.s.i. compression. If specimens of this type are conventionally shot peened, the expected residual compressive stress, which is greater than that from presetting, is introduced, and an associated increase in the endurance limit may be noted. Still higher residual compressive stresses are introduced if specimens are strain peened in tension. This results in a still higher endurance limit (approximately 194 k.s.i. for the + 0.60% strain-peening and 176 k.s.i. for the + 0.30% strain peening). While the benefits of tensile strain peening have been known for many years this process has not been used extensively in practice. The present study is the first time, to our knowledge, that strain peening under conditions of compression has

References p. 357.

been tried. If specimens are subjected to compressive strain during peening, residual tensile stresses may be introduced near the surface. For a strain peening of 0.60% compression the peak residual stress in the affected surface layer is approximately 60 k.s.i. tension and the endurance limit drops to approximately 55 k.s.i.

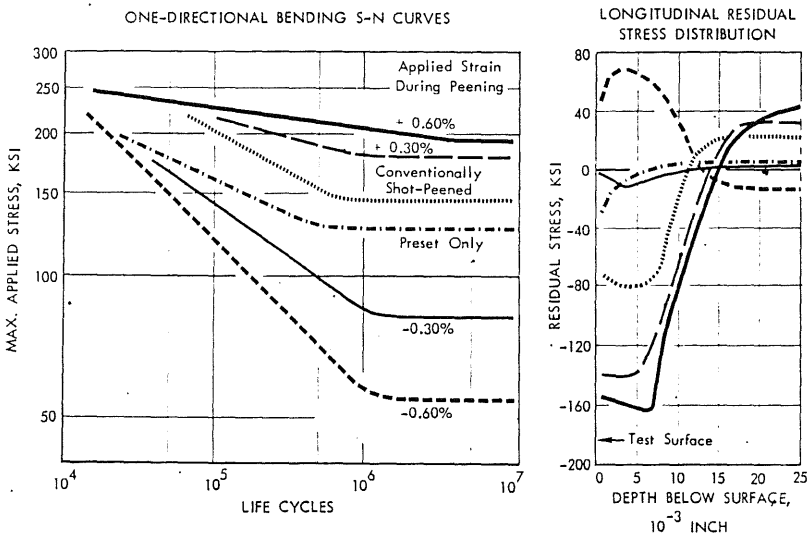

Fig. 8. S–N curves and residual stresses for variously shot-peened leaf-springs.

This is a drastic drop. An intermediate result is obtained with –0.30% strain peening. It is reasonable to assume that the effects of strain hardening on all five shot-peened groups were about the same, since the total local strain caused by the impact of shot particles is obviously many times greater than the applied elastic strain during strain peening. Yet the endurance limits are drastically different. The primary differences observed are found in the residual stress distributions shown on the right-hand diagram. This is considered to be the most important observation made in this study. If strain hardening were the more dominant feature of the shot-peening process, the endurance limits would have been more nearly the same.

A conventional AM (alternating stress *versus* mean stress) plot of these fatigue data would show how illogical it is to consider fatigue test results of this kind without considering the residual stress state. Such a plot would have a positive slope and go through the origin. It is quite clear that as the mean stress goes to zero the varying stress would also have to go to zero, which, of course, is completely incorrect. However, if the residual stress is taken into account, and, as a first approximation consideration is given only to stress near the surface, a much more reasonable line would be obtained.

References p. 357.

In Fig. 9 the endurance limit is plotted against residual stress near the test surface. For all of the specimens which were shot peened, it can be seen that there is an approximately linear relationship. In addition, the "preset only" specimen actually lies to the right of the curve, indicating that for the same level of residual

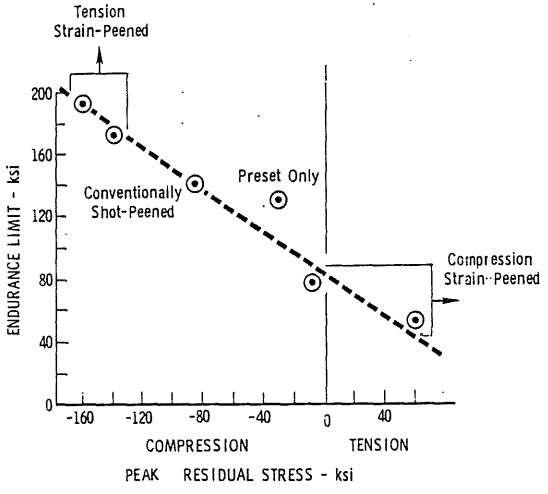

Fig. 9. One-directional bending endurance limit as a function of peak residual stress near the test surface.

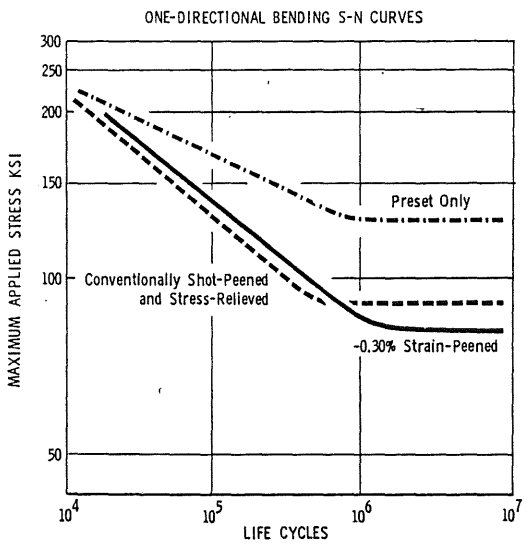

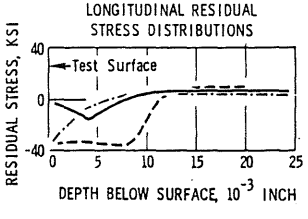

TEST SURFACE ROUGHNESS AND HARDNESS VALUES

TEST GROUP	SURFACE ROUGHNESS	HARDNESS ROCKWELL "C"
Preset Only	7-12	48
-0.30% Strain-Peened	120-140	51
Conventionally Shot-Peened and Stress-Relieved	120-140	48

Fig. 10. Separate effects of surface roughness and residual compressive stress on fatigue properties.

References p. 357.

stress the endurance limit is somewhat higher. This is attributed to the smoother surface, and/or a more beneficial type of strain hardening from the presetting operation.

Figure 10 illustrates the influence of surface roughness. Conventionally-peened specimens were given a stress-relief treatment of 2–1/2 h at 650 °F and then fatigue tested, giving the results shown. The stress-relief treatment did not alter the hard-

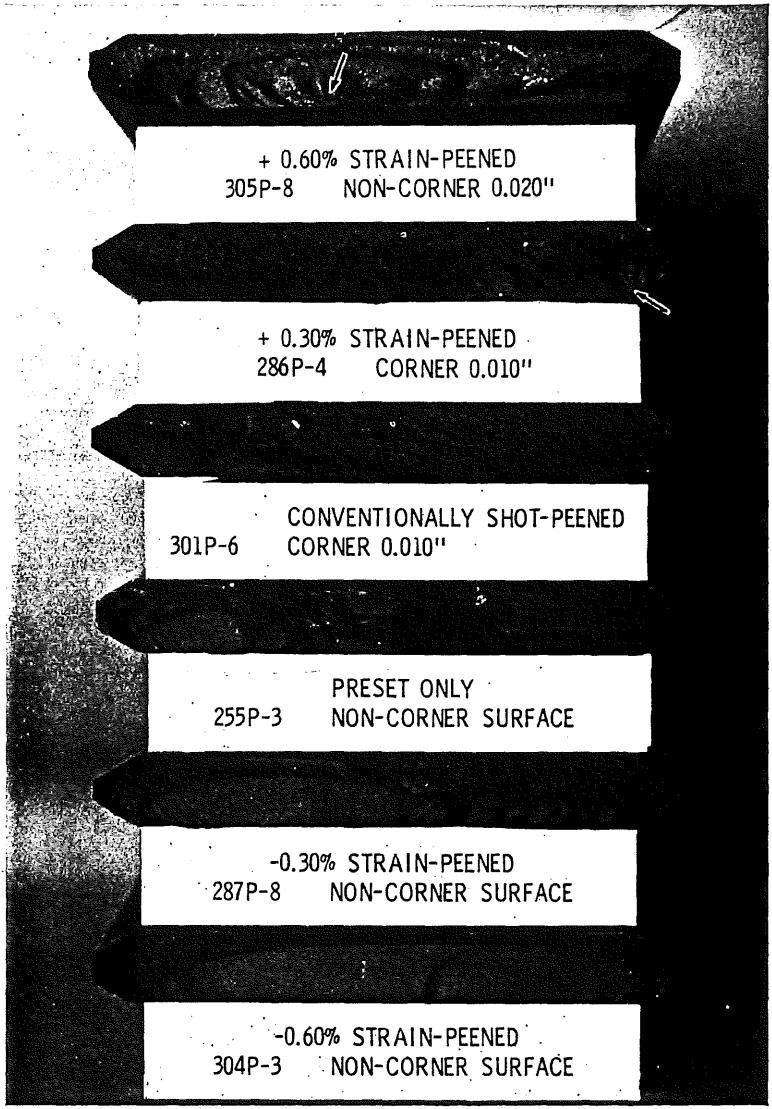

Fig. 11. Fatigue fractures of leaf-spring specimens showing fatigue failure origins.

References p. 357.

ness significantly, but the endurance limit dropped from 146 k.s.i. to 92 k.s.i. Residual stress analyses showed that the shot-peened, stress-relieved specimens had about the same residual stress near the surface as the "preset only" group (*i.e.* —35 k.s.i.) as can be seen in Fig. 10. Yet the, "shot-peened, stress-relieved" group gave a much lower endurance limit, which, primarily, can be attributed to the increased surface roughness. When the "shot-peened, stress-relieved" group is compared with the group peened at an applied strain of —0.30%, which has similar

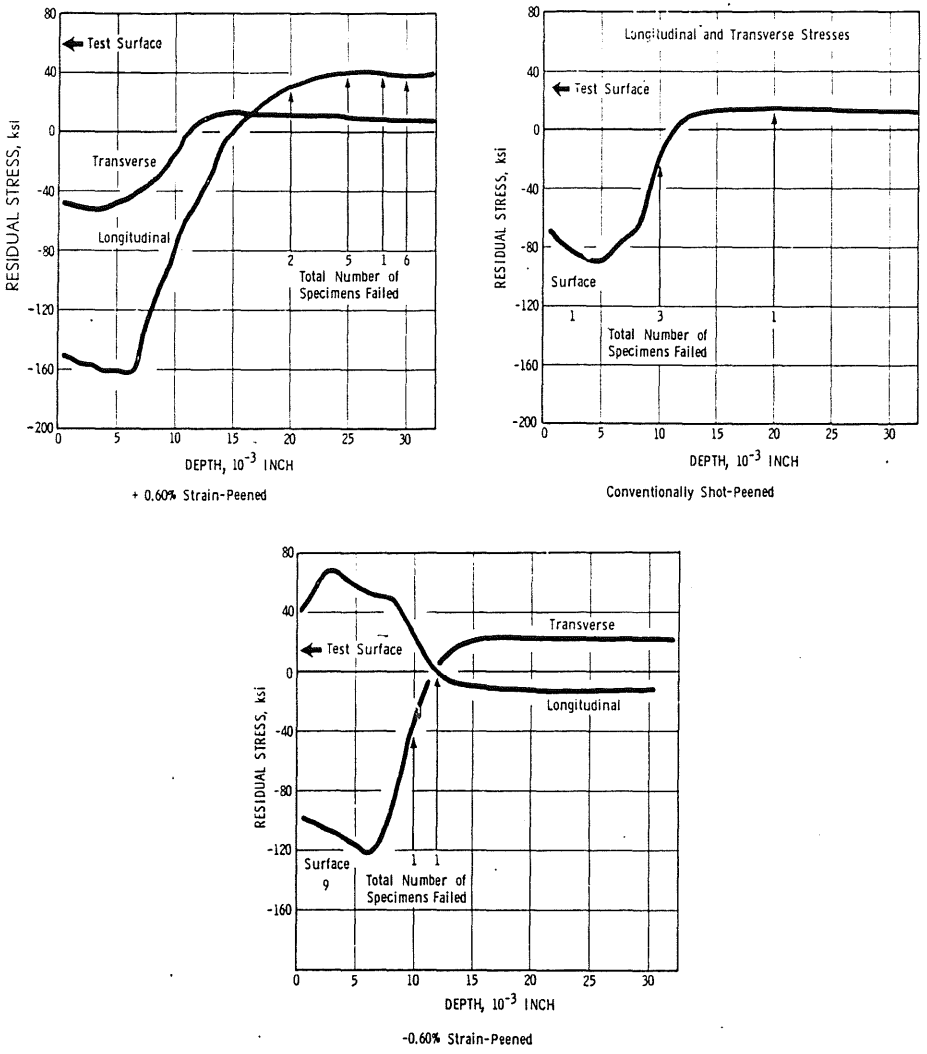

Fig. 12. Locations of fatigue failure origins and residual stress distributions.

References p. 357.

surface roughness, the difference can probably be accounted for by the more favorable residual stress in the "shot-peened, stress-relieved" group. A further comparison can be made between the "shot-peened, stress-relieved" group and the "as heat-treated" group. Here, in spite of increased surface roughness, the "shot-peened, stress-relieved" group has a higher endurance limit than the "as heat-treated" group. However, the "shot-peened, stress-relieved" group has a more favorable residual stress near the surface, which may account for this observation.

While the linear relationship of the peak residual stress in the affected surface layer and endurance limit shown by Fig. 9 looks impressive, its real meaning is somewhat clouded by the fact that specimens which were tensile strain peened had their origins of failure below the surface where the stress state was quite different (see arrows, Fig. 11). The same applies to specimens which were shot peened under compressive strain, which actually showed evidence of failure near the surface. Furthermore, extension of the curve to the point of zero endurance limit indicates a mean stress of about 110 k.s.i. Since the yield strength is nearly twice that much, this does not seem to be realistic. Because of these points, a more thorough analysis was made of the residual stresses in depth in both the longitudinal and the transverse direction of three types of specimens: (1) peened under 0.60% tension, (2) conventionally shot peened, and (3) peened under 0.60% compression. Results are shown by Fig. 12, which also gives failure locations. Incidentally, measurements of residual stresses were made both before fatigue testing and after fatigue testing at loads corresponding with endurance limit. These revealed little or no change occurring in the macro residual stress distribution because of the fatigue cycling.

Correlation with failure criteria

From biaxial residual stress data and the endurance limits observed, it was possible to examine the results in relation to various failure criteria. Consideration was given to the maximum stress theory, the distortion energy theory and the maximum shear stress theory.

Residual stresses and load stresses were added algebraically (superpositioned). Longitudinal stresses and transverse stresses were considered separately to determine the combined stress state under conditions of endurance limit loading for each of the three groups of specimens (+ 0.60% strain peened, conventionally shot peened, and −0.60% strain peened). The results are plotted in Figs. 13, 14 and 15. The three groups are combined in Fig. 16 for purposes of comparison. In each of the individual diagrams the biaxial stress state under conditions of no-load and full-load are shown for near the surface and for various points beneath the surface. The length of the horizontal element in each of these envelopes represents the stress range at the endurance limit. (In the experimental method of fatigue testing used, the transverse stress due to applied load is zero.) The loci of the minimum and

References p. 357.

maximum stresses for each case show relative nearness to the critical stress states defined by each of the three theories.

For purposes of reference the yield point ellipse based upon the distortion energy criterion is shown in true scale. A geometrically similar ellipse should be considered for fatigue, but its scale value is not known. The maximum shear stress diagram and the maximum stress diagram are also shown, but neither of these is the true scale since the true values are not known.

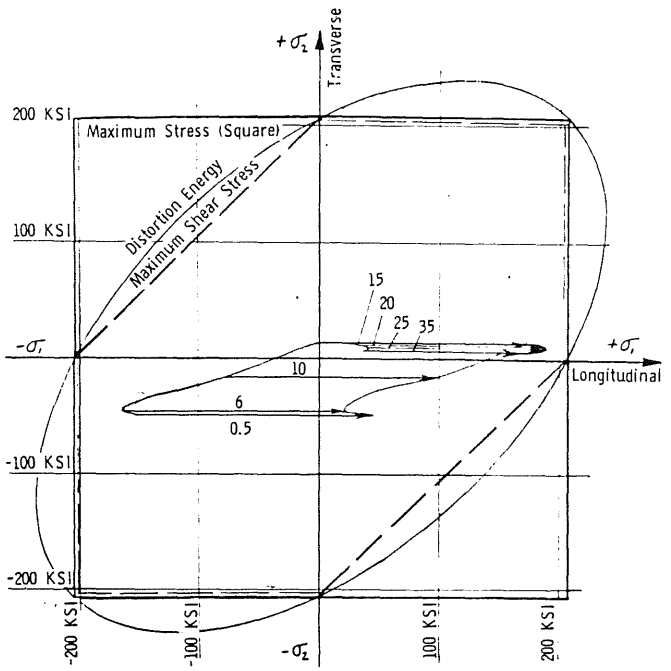

Fig. 13. Failure criteria and biaxial stresses resulting from superpositioning of residual and endurance limit stresses for +0.60% strain-peened group. Stresses are shown for various depths below the surface. (Distance below the surface in 1/1000 inch is indicated by the numerals on the stress envelope.)

Considering the maximum stress theory, only stress in a longitudinal direction need be considered. Here, as can be seen from Fig. 16, the tensile-peened group should be the weakest and the compressive-peened group the strongest, yet it is obvious that the opposite is true.

According to the maximum shear stress theory the compressive-peened group should be, and is, the weakest, but the conventionally shot-peened group should be the strongest, and it is not. Its strength is greatly exceeded by the tensile-peened group.

References p. 357.

For the distortion energy criteria the predicted order of strength would be: compressive-peened weakest, tensile-peened next and conventionally peened strongest.

Consideration must be given, however, to possible variations in strength through the cold-worked layer. Predictions would be hazardous, but to satisfy both the

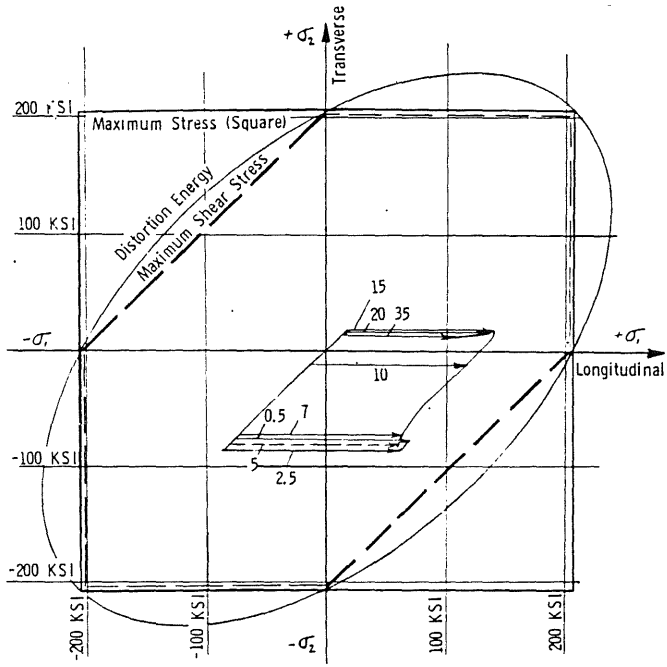

Fig. 14. Failure criteria and biaxial stresses resulting from superpositioning of residual and endurance limit stresses for conventionally shot-peened group. Stresses are shown for various depths below the surface. (Distance below the surface in 1/1000 inch is indicated by the numerals on the stress envelope.)

distortion energy theory and the maximum shear stress theory the material would have to be weaker at an intermediate depth than either the region near the surface (0 to 0.005 in. depth) or the region immediately below the cold-worked layer (0.025 in. to 0.030 in.). This seems highly improbable.

To satisfy the maximum tensile stress theory the strength of the material below the cold-worked layer would have to be stronger than that within the cold-worked layer. This likewise seems improbable.

Considering all three theories, it appears that either the distortion energy theory or the maximum shear stress theory would satisfy the results better than the maximum stress theory. Both the tensile-peened group and the compressive-peen-

References p. 357.

ed group are satisfied by these theories. Only the conventionally shot-peened group is not. It may be that better correlation would be obtained if the stress perpendicular to the surface were considered. Furthermore, the maximum stress theory predicts results opposite to those observed.

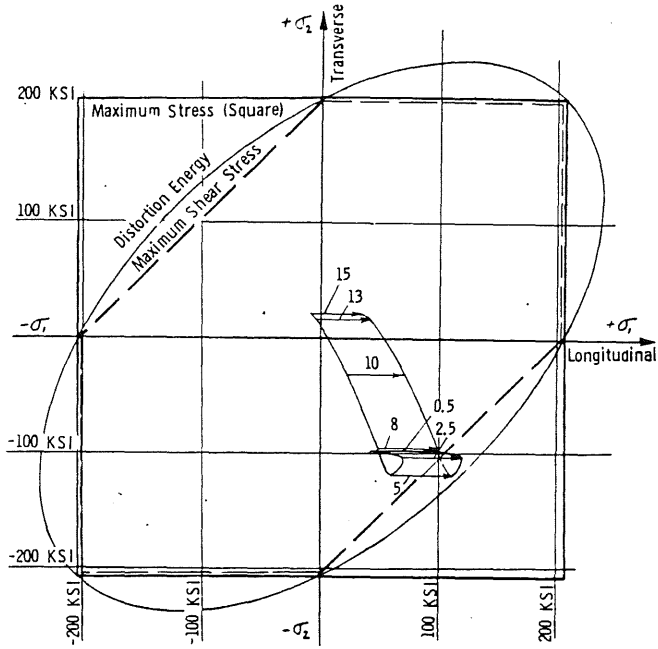

Fig. 15. Failure criteria and biaxial stresses resulting from superpositioning of residual and endurance limit stresses for —0.60% strain-peened group. Stresses are shown for various depths below the surface. (Distance below the surface in 1/1000 inch is indicated by the numerals on the stress envelope.)

It is also interesting to note that the failure origins are located subsurface for the tensile strain-peened group, as would be predicted by all three theories, and this might be expected if the surface is "protected" by a compressed layer. All compressive strain-peened specimens had their origins at or very near the surface, as would be expected from the failure theories. The conventionally shot-peened group had origins at various locations, as might be predicted by either the maximum shear stress theory or the distortion energy theory.

It is to be noted, however, that the closer the mean stress is to the critical stress for each of the failure criteria, the narrower is the permissible alternating stress. For example, the compressive-peened group has a low alternating stress, and its mean stress is very close to the yield ellipse. The conventionally peened and the

References p. 357.

tensile-peened follow in that order if conditions of stress near the surface are considered. This is not clearly true beneath the surface, but variations in strength may be responsible for this divergence.

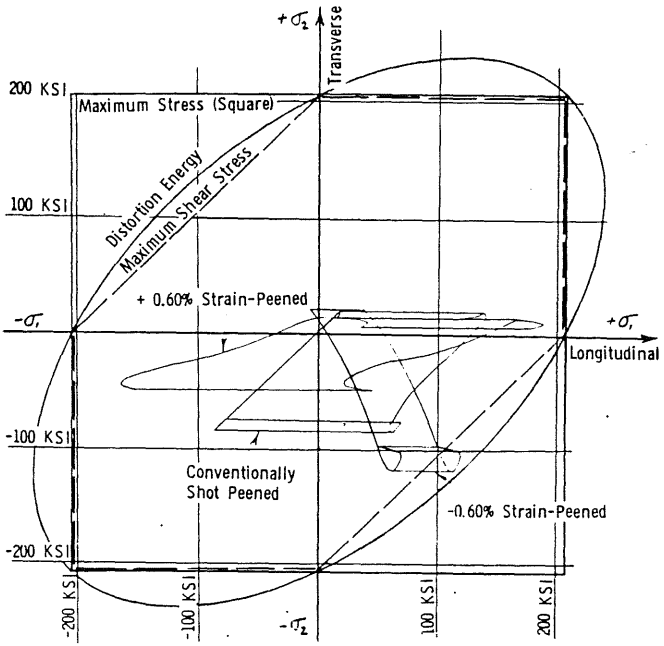

Fig. 16. Combined biaxial stress diagrams of three groups: +0.60% strain-peened, conventionally shot-peened, and −0.60% strain-peened, taken from Figs. 13, 14, and 15.

CONCLUSIONS

For the material, specimen, and testing described in this experiment, the following conclusions are drawn:

1. Good correlation was found between endurance limits and the residual stress state near the surface independent of any work-hardening influence. This supports the concept of superpositioning of residual stresses and load stresses. True quantitative interpretation was not possible with the limited data, but none of the results contradict the idea of considering residual stresses as being additive to mean load stresses.

2. It appears from this investigation that shot peening steel of this hardness is indeed beneficial primarily because of the introduction of the macro residual compressive stress. There is no gain attributable to "strain hardening" for this material. There is some indication that the increased surface roughness caused by shot peening is harmful to fatigue strength.

References p. 357.

3. Fair correlation was found between endurance limits and the distortion energy criterion and the maximum shear stress criterion of failure, using the principle of superpositioning of residual stress and load stresses and failure locations.

REFERENCES

1 T. J. DOLAN, B. J. LAZAN AND O. J. HORGER, *Fatigue*, American Society for Metals, Cleveland, 1954, p. 25.
2 Attention is directed to *U. S. Patent No. 2,608,752*.
3 J. O. ALMEN, Fatigue weakness of surfaces, *Product Eng., 21* (1950) 125; and private communications.
4 R. L. MATTSON AND W. S. COLEMAN, JR., Effect of shot peening variables and residual stresses on the fatigue life of leaf spring specimens, *S.A.E. Trans., 62* (1954) 548.
5 L. G. JOHNSON, Derivation of the fundamental equation of residual stress analysis by dissection, *Ind. Math., 5* (1955) 7.
6 L. G. JOHNSON, The effect of slicing on residual stresses in plates, *Ind. Math. Soc., 3* (1952) 42.

Appendix

FATIGUE TEST RESULTS

Specimen No.	*Max. applied stress (k.s.i.)*	*Change in max. stress at 10,000 cycles*		*Location of failure origin*			*Life cycles*
		Change (k.s.i.)	*% of original stress*	*Corner*	*Noncorner*	*Depth (inches)*	
+ 0.60% Strain peened							
305P–1	197.7	— 4.4	—2.2	No failure			11,881,540
305P–2	204	—16.7	—8.2		×	0.030	2,182,900
305P–3	207	— 2.0	—1.0		×	0.030	3,013,000
305P–4	190	— 4.0	—2.1		×	0.030	2,109,800
305P–5	195	— 4.4	—2.3		×	0.020	2,370,100
305P–6	206	— 2.5	—1.2	×		0.030	3,095,750
305P–7	198	— 0.6	—0.3		×	0.025	2,288,000
305P–8	200	— 0.6	—0.3		×	0.020	1,150,060
302P–1	202.7	+12.8	+6.3		×	0.025	1,781,430
302P–2	202.3	+12.2	+6.0		×	0.025	1,381,410
302P–3	194.6	— 0.6	—0.3	No failure			10,907,000
302P–4	209	— 0.6	—0.3		×	0.025	1,578,690
302P–5	210	— 1.1	—0.5	×		0.025	1,261,040
302P–6	224	— 3.6	—1.6		×	0.030	135,500
302P–7	224	— 2.8	—1.2		×	0.030	148,430
302P–8	194.3	0	0		×	0.028	2,437,530
+ 0.30% Strain peened							
286P–1	202.7	— 1.1	—0.5	×		0.005 – 0.008	114,000
286P–2	201.5	— 1.1	—0.5	×		0.010 – 0.012	149,200
286P–3	180.6	— 1.1	—0.6	No failure			966,700
286P–4	187.7	— 0.6	—0.3	×		0.010 – 0.012	561,800
286P–5	188.1	— 1.1	—0.6	×		0.018	533,500
286P–6	180	— 1.1	—0.6		×	0.020	7,206,900
286P–7	200.3	— 0.6	—0.3	×		0.020	297,500
286P–8	201.9	— 1.4	—0.7	×		0.014	195,200
Conventionally shot peened							
301P–1	199	— 1.7	—0.9		×	Surface	103,100
301P–2	200	— 0.8	—0.4	×		0.020 – Surface	119,800
301P–3	149.5	0	0	No failure			3,162,400
301P–4	157.2	— 0.6	—0.4	×		0.020	207,300

Specimen No.	*Max. applied stress (k.s.i.)*	*Change in max. stress at 10,000 cycles*		*Location of failure origin*			*Life cycles*
		Change (k.s.i.)	*% of original stress*	*Corner*	*Noncorner*	*Depth (inches)*	
301P–5	156	− 0.6	−0.4	×		0.010	259,900
301P–6	150	+ 0.3	+0.2	×		0.010	308,000
301P–7	147	+ 0.3	+0.2	×		0.010	543,900
301P–8	142	0	0	No failure			4,170,000
Preset only							
224P to 229P (45 Specimens)	200 (Nominal)	0 to −1.4	0 to −0.7	21 Specimens	24 Specimens	Surface	22,450 (Average)
255P–1	143.5	−0.3	−0.2		×	Surface	140,500
255P–2	122	+0.3	+0.2	No failure			7,933,300
255P–3	129	+0.3	+0.2		×	Surface	409,300
255P–4	122.6	+0.3	+0.2	No failure			3,638,000
255P–5	128	+3.1	+2.4		×	Surface	934,500
255P–6	130	+0.3	+0.2	No failure			1,620,100
255P–7	136.5	−0.6	−0.4	×		Surface	7,536,700
255P–8	127	+0.6	+0.5		×	Surface	7,745,500
Shot peened and stress relieved							
327P–8	201	−0.4	−0.2		×	Surface	12,100
327P–7	199.8	−0.4	−0.2		×	Surface	12,700
327P–5	202.1	−1.1	−0.5		×	Surface	13,700
327P–6	200.3	−0.6	−0.3		×	Surface	14,100
327P–1	202	−1.1	−0.5		×	Surface	14,600
327P–4	200.3	−0.8	−0.4		×	Surface	15,600
327P–3	202	−1.6	−0.8		×	Surface	16,000
327P–2	202.3	−2.8	−1.4		×	Surface	17,400
328P–7	103.2	0	0		×	Surface	103,200
328P–2	103.6	0	0		×	Surface	240,800
328P–5	97.4	0	0	×		Surface	273,400
328P–6	97.1	0	0		×	Surface	385,500
328P–1	97.5	0	0		×	Surface	393,200
328P–3	83.8	0	0	No failure			10,040,300
328P–4	89.8	0	0	No failure			12,474,400
As heat treated							
316P–3	203	−2.5	−1.2		×	Surface	14,350
316P–8	203	−1.7	−0.8		×	Surface	15,400
316P–4	203	−2.0	−1.0		×	Surface	15,900
316P–7	203	−2.8	−1.4		×	Surface	16,050
316P–1	201	−2.8	−1.4	×		Surface	16,100
316P–2	199	−1.6	−0.8		×	Surface	16,300
316P–5	203	−1.1	−0.5	×		Surface	16,600
316P–6	197	−3.1	−1.6		×	Surface	19,500
317P–2	148	−0.3	−0.2	×		Surface	56,800
317P–1	162.5	+0.6	+0.4		×	Surface	57,100

Specimen No.	Max. applied stress (k.s.i.)	Change in max. stress at 10,000 cycles		Location of failure origin			Life cycles
		Change (k.s.i.)	% of original stress	Corner	Noncorner	Depth (inches)	
317P–4	134	−1.4	−1.0	×		Surface	69,700
317P–3	140.5	−1.4	−1.0		×	Surface	90,100
317P–5	119	−1.1	−0.9		×	Surface	113,400
317P–7	90.8	−0.3	−0.3		×	Surface	199,300
318P–8	113	−1.7	−1.5	×		Surface	244,100
318P–5	106	−0.8	−0.8		×	Surface	328,100
317P–8	82.9	−0.3	−0.4		×	Surface	437,400
317P–6	97.9	−0.6	−0.6		×	Surface	703,600
318P–3	85.0	−0.3	−0.4	No failure			9,507,600
318P–6	99.4	−0.8	−0.8	No failure			10,000,190
318P–4	91.3	−0.6	−0.7	No failure			10,263,200
318P–7	106	−1.1	−1.0	No failure			10,547,700
318P–2	77	−0.6	−0.8	No failure			10,560,800
−0.30% Strain peened							
287P–1	200.2	−7.0	−3.5		×	0.005	23,250
287P–2	200.5	−7.5	−3.7		×	Surface	23,800
287P–3	179.3	−4.2	−2.3		×	Surface	40,400
287P–4	158.0	−3.3	−2.1		×	Surface	44,480
287P–5	158.4	−4.2	−2.7		×	Surface	41,100
287P–6	116.8	−1.1	−0.9		×	Surface	169,700
287P–7	88.8	−1.1	−1.2		×	Surface	770,300
287P–8	81.9	−1.4	−1.7		×	Surface	834,500
−0.60% Strain peened							
303P–1	201.5	−14.5	−7.2		×	0.010	18,100
303P–2	201.2	−15.0	−7.4		×	Surface	19,600
303P–3	75.4	−0.8	−1.1		×	Surface	385,700
303P–4	76.7	−1.7	−2.2		×	Surface	391,500
303P–5	50.1	−1.9	−3.8	No failure			7,198,800
303P–6	64.0	−1.1	−1.7		×	Surface	977,900
303P–7	56.3	−1.7	−3.0	No failure			11,670,850
303P–8	64.0	−1.9	−3.0		×	Surface	649,200
304P–1	98.6	−7.6	−7.7		×	0.012	144,200
304P–2	74.3	−4.8	−6.5		×	Surface	476,000
304P–3	66.5	−3.0	−4.5		×	Surface	871,900
304P–4	59.0	−1.4	−2.4		×	Surface	790,800
304P–5	53.1	−2.0	−3.8		×	Surface	3,060,000
304P–6	51.0	−1.1	−2.2	No failure			10,000,000
304P–7	75.6	−1.9	−2.5	No failure			11,668,900
304P–8	76.4	−0.6	−0.8	No failure			10,692,900